Origin of the increased resistivity in epitaxial Fe_3O_4 films

W. Eerenstein,* T. T. M. Palstra, and T. Hibma

Material Science Center, University of Groningen, Nijenborgh 4, 9747 AG Groningen, The Netherlands

S. Celotto

Department of Engineering, Materials Science and Engineering, University of Liverpool, Brownlow Hill,
Liverpool L69 3BX, United Kingdom

We report resistivity measurements on epitaxial Fe_3O_4 films between 3 and 100 nm thickness grown on polished MgO substrates. The resistivity of the films is larger than the bulk resistivity, and is increasing with decreasing film thickness. This can be explained by the significant decrease of antiphase domain size with decreasing film thickness, as observed by transmission electron microscopy. The domain size decreases from 40 nm for 100-nm-thick films, to 5 nm for 3-nm-thick films. The effective conductivity has been modeled as a function of the bulk and boundary conductivities using the effective medium approximation. It is suggested that the absence of the Verwey transition in the thinnest films is also related to the very small domain size, which inhibits long-range order.

Magnetite films have received a lot of attention due to the combination of several interesting properties. These are the highly spin-polarized conduction electrons,[1] the high Curie temperature of 858 K, and the fact that these films show magnetoresistance behavior.[2,3] Epitaxial thin films of Fe_3O_4 are known to exhibit an increased resistivity with respect to the resistivity of a bulk crystal. Furthermore, the resistivity of these films increases with decreasing film thickness.[4,5] In this paper we will show that this behavior is related to the presence of a high density of antiphase boundaries (APB) in thin, epitaxial magnetite films.[3,6,7] The antiphase boundaries are formed as growth defects, due to the fact that the lattice constant of Fe_3O_4 is twice as large as the lattice constant of the underlying substrate, MgO.[7,8] When different islands meet, they can be shifted or rotated with respect to each other, thus yielding an antiphase boundary. At some of these antiphase boundaries, 180 deg superexchange interactions are present, which are not present in bulk Fe_3O_4. This superexchange interaction is antiferromagnetic. Due to the high degree of spin polarization in Fe_3O_4, the presence of these antiferromagnetic boundaries enhances the resistance of these films. This explains the increase in resistivity with respect to bulk Fe_3O_4.

In this paper we report on the thickness dependence of the resistivity and its relationship with changes in the domain structure for films of 3, 6, 12, 25, 50, and 100 nm thickness. The epitaxial Fe_3O_4 films were grown on polished magnesium oxide (MgO) substrates using molecular beam epitaxy in an ultrahigh vacuum system with a background pressure of 10^{-10} mbar. During deposition, an oxygen pressure of 10^{-6} mbar and an iron flux of 1.25 Å/min were employed. For the resistivity measurements, four contacts were made by depositing 20 nm of Ti and 40 nm of Au. Resistance measurements were performed in a physical property measurement system (PPMS) by Quantum Design. To study the films with transmission electron microscopy (TEM), specimens were prepared by floating the Fe_3O_4 films off the MgO substrates in a 4 wt % ammonium sulfate solution at 70 °C (343 K).[9]

The resistivity of the films vs $1/T$, with T the temperature, is shown in Fig. 1. The thinnest film, the 3-nm-thick film, has the highest resistivity that is 30 times larger at room temperature (RT) than the bulk resistivity of 4 mΩ cm.

The resistivity decreases as the film thickness increases. This phenomenon has also been observed for Fe_3O_4 films grown by pulsed laser deposition.[4] Because the resistance of the films is enhanced with respect to the bulk due to the presence of anti phase domain boundaries, it is anticipated that the size of the domains varies with film thickness. Dark field TEM images of the 3-, 6-, 12- and 25-nm-thick films are shown in Fig. 2. These images have been recorded using the spinel (220) reflection near the [001] zone axis, and the dark lines are the antiphase boundaries with a
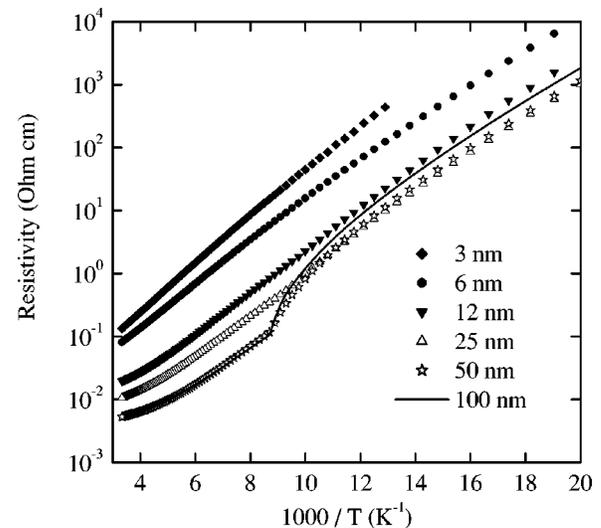

FIG. 1. Resistivity vs 1/T of 3, 6, 12, 25, 50, and 100-nm-thick epitaxial Fe_3O_4 films on MgO. The resistivity of the 3-nm-thick film is 30 times larger than the resistivity of the 50-nm-thick film. Only the 50-nm- and 100-nm-thick films show a Verwey transition, which is broadened and lowered with respect to the bulk.
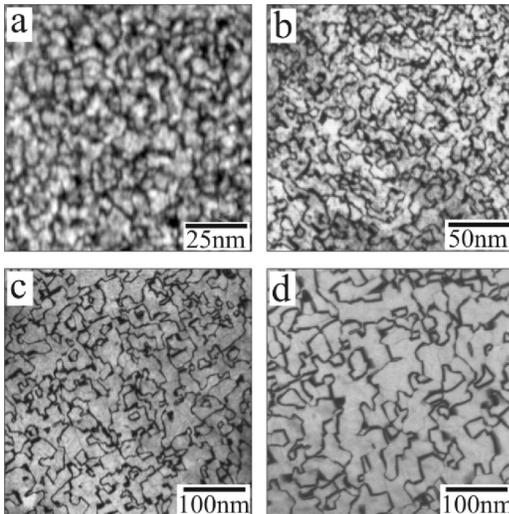
FIG. 2. Dark field transmission electron micrographs of Fe_3O_4 films on MgO, with thicknesses (a) 3 nm, (b) 6 nm, (c) 12 nm, and (d) 25 nm. Images were taken with the (220) reflection near the [001] zone axis.

$1/4[011], 1/4[01\bar{1}], 1/4[101], 1/4[10\bar{1}]$ shift (note that the $1/4[110]$, $1/4[1\bar{1}0]$, and $1/2[100]$ are out of contrast). Figure 2 shows that the domain size increases with increasing film thickness. Note also that the domain size for a given thickness is rather uniform.

The average domain sizes have been determined by the linear intercept method, i.e., from the number of line crossings. The obtained value for the domain size is, however, too large, because only four out of the seven possible APB shifts are visible in the dark field image when using the (220) reflection.

To obtain the actual domain size, these values thus have to be multiplied by a factor 4/7. The domain sizes and corresponding film thicknesses are shown in the first two columns of Table I. The domain size increases from 5 nm for the 3-nm-thick film to 40 nm for the 100-nm-thick film. The domain sizes D vs film thickness h are plotted in Fig. 3(a). We observe that $D \propto \sqrt{h}$ and thus $D \propto \sqrt{t}$, with t being the deposition time.

From Fig. 2 it becomes clear that the APB's are not simply formed in the first layer during deposition and continue
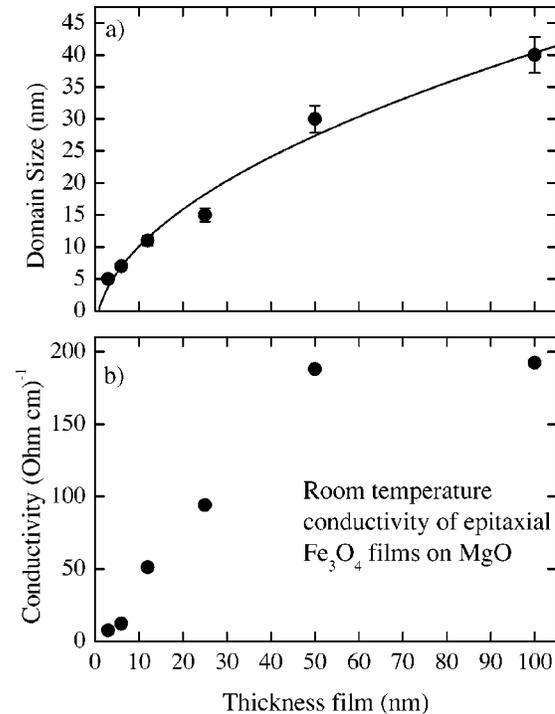

FIG. 3. Structural and electronic properties of 3-, 6-, 12-, 25-, 50-, and 100-nm-thick Fe_3O_4 films: (a) Structural domain size obtained from dark field TEM. The solid line is a fit $D \propto \sqrt{h}$. (b) Room-temperature conductivity.

to grow through the film as more material is deposited. Rather, it appears that the domains grow in time by a diffusive motion of the APB. The cause of this effect is probably that the domain boundaries are high-energy areas and the energy of the system can be reduced when the total domain-wall area is reduced. The increase in domain size is surprising and no explanation for the growth of domain size with film thickness exists so far. Further studies are underway to determine the nature of this phenomenon.

Figure 3(b) shows the room-temperature conductivity (i.e., 1/resistivity) vs film thickness. The conductivity increases from 7.5 $(\Omega \, cm)^{-1}$ for the 3-nm-thick film to 192 $(\Omega \, cm)^{-1}$ for the 100-nm-thick film. From Figs 3(a) and 3(b) it is thus clear that as the domain size increases with film thickness, so does the conductivity. The conductivity

TABLE I. Structural domain size, RT resistivity, RT conductivity, and volume fraction of bulk phase for different film thicknesses of Fe_3O_4 films on MgO.

Film thickness (nm)	Domain size (nm)	Resistivity (Ω cm)	Conductivity (Ω cm)$^{-1}$	ϕ_b
3	5	0.13	7.6	0.36
6	7	0.082	12.2	0.51
12	11	0.017	58.8	0.67
25	20	0.008	119	0.81
50	28	0.0053	189	0.86
100	40	0.0052	192	0.90

sharply increases for the thinnest films, and has nearly approached the bulk value for the two thickest films (50 nm and 100 nm). The resistivities and conductivities are shown in the third and fourth columns of Table I.

Thus far, the effective conductivity σ_e of Fe_3O_4 films containing antiphase boundaries was not known and assumed to be an (unknown) function of the bulk conductivity σ_b and the boundary conductivity σ_{APB}.[3] A suitable model to describe the total conductivity is the effective medium approximation (EMA) for a two-phase composite, which was originally derived by embedding a circular inclusion into a homogeneous medium.[10] Torquato and Hyun have shown[11] that the EMA is also valid for a two-dimensinal dispersion of inclusions characterized by a single length. In case of two-dimensional inclusions, the EMA equation for the effective conductivity σ_e (Ref. 11) is

$$\phi_b\left(\frac{\sigma_e-\sigma_b}{\sigma_e+\sigma_b}\right)+\phi_{APB}\left(\frac{\sigma_e-\sigma_{APB}}{\sigma_e+\sigma_{APB}}\right)=0, \quad (1)$$

where ϕ_b and ϕ_{APB} are the volume fractions of the bulk and antiphase boundary phases, such that $\phi_b+\phi_{APB}=1$. If we
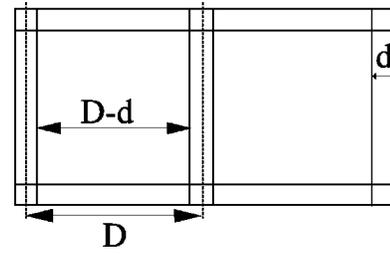

FIG. 4. Schematic drawing of domain structure, with finite domain boundary width d.

assume square shaped domains with an average size D and a domain boundary of thickness d (see in Fig. 4) ϕ_b can be calculated as

$$\phi_b=\frac{(D-d)^2}{D^2}=\left(1-\frac{d}{D}\right)^2. \quad (2)$$

Inserting $\phi_{APB}=1-\phi_b$ into Eq. (1), we obtain for the effective conductivity

$$\sigma_e=0.5[(\sigma_b-\sigma_{APB})(2\phi_b-1)+\sqrt{(\sigma_b^2+\sigma_{APB}^2)(2\phi_b-1)^2+2\sigma_b\sigma_{APB}(2-(2\phi_b-1)^2)}]. \quad (3)$$

The conductivity vs $1/D$ at RT and 150 K is shown in Figs. 5(a) and 5(b), respectively. The solid lines are fits using Eq. (3). The obtained values at room temperature are $\sigma_b=260\pm12\ (\Omega\ cm)^{-1}$, $\sigma_{APB}=2\pm2.3\ (\Omega\ cm)^{-1}$, and the boundary width $d=2$ nm±0.2, and at 150 K they are $\sigma_b=58\pm4\ (\Omega\ cm)^{-1}$, $\sigma_{APB}=0.8\pm0.7\ (\Omega\ cm)^{-1}$, and $d=3$ nm±0.4. The obtained values for the bulk conductivity are in excellent agreement with the bulk values of 250 and 50 $(\Omega\ cm)^{-1}$ at RT and 150 K, respectively. The value for the boundary width is very reasonable compared to the linewidth of the boundaries in Fig. 2, from which d is estimated to be 1–3 nm. Inserting $d=2$ nm in Eq. (2), ϕ_b has been calculated and these values are shown in the last column of Table I.

The value for σ_{APB} is very small. Indeed, the conductivity at the boundary is expected to be zero in the case of perfect antiferromagnetic coupling at the boundaries.[3] In reality, the boundary conductivity is small, but finite, since several configurations are possible at the boundaries[7] and the magnetic coupling may be frustrated to some extent.[8] If $\sigma_{APB}\ll\sigma_b$, Eq. (3) may be approximated as

$$\sigma_e=\sigma_b(2\phi_b-1) \quad (4)$$

as long as $\phi_b>0.5$. Neglecting the quadratic term in d/D in Eq. (2), this expression represents a straight line. From Fig. 5 it is evident that it is a very good approximation for the films having a bulk fraction ϕ_b well above 0.5.

Near and below $\phi_b=0.5$, the full expression [Eq. (3)] should be used. For $\phi_b=0.5$, Eq. (3) reduces to $\sigma_e=\sqrt{\sigma_b\sigma_{APB}}$, the geometric mean of the two components.
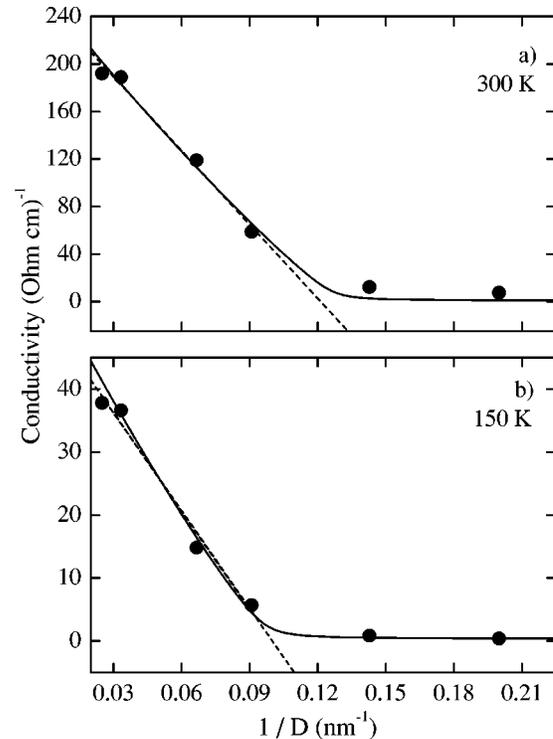

FIG. 5. Conductivity vs $1/D$ (D stands for domain size in nanometers) for 12-, 25-, 50-, and 100-nm-thick Fe_3O_4 films (a) at room temperature and (b) at 150 K. The solid lines are fits using Eq. (3), the dashed lines are fits using Eq. (4).

The small but finite value for σ_{APB} is therefore related to the conductivity for $\phi_b < 0.5$. It should be noticed, however, that the EMA is not very accurate around $\phi_b = 0.5$, because the percolation problem is not properly treated. In addition, our model of the domain structure is breaking down in this region. Consequently, the value for σ_{APB} obtained from the fit should not be given too much importance, except that it is low and close to zero.

Also noteworthy is the absence of the Verwey transition for the thinnest films (25 nm and below) and a lower T_v for 50- and 100-nm-thick films (see Fig. 1). Epitaxial stress and a structural coupling between the film and the substrate have been suggested as possible origins of these effects.[5] However, also Fe_3O_4 films on $MgAl_2O_4$, which are relaxed because of the large misfit (4%) show similar resistivity behavior. The resistivity is also increased with respect to the bulk and is thickness dependent.[5,12] Fe_3O_4 films on $MgAl_2O_4$ also exhibit an APB network.[12] Therefore, it is more likely that the domain structure causes the absence of the Verwey transition.

As was pointed out by Ihle and Lorenz,[13] both electron correlation and electron-phonon interactions play a role in the conductivity behavior of Fe_3O_4. For the Verwey transition to occur, long-range order of the Fe^{2+} and Fe^{3+} ions at the octahedral lattice sites is necessary. Recently Wright *et al.*[14] have obtained direct crystallographic evidence for long-range ordering on the octahedral iron sites. The epitaxial films contain a high density of APB, and at these boundaries the nearest-neighbor configuration is disturbed. In fact, the domain size for the 3-nm-thick film is so small that the domains consist only of a few unit cells. This very small domain size can inhibit long-range order.

Ultrathin Fe_3O_4 films also have a vanishing remanent magnetization and in-plane anisotropy below a thickness of 10 nm.[15] For thicker films, the in-plane anisotropy resembles the bulk anisotropy with [110] as the easy direction. The reduction of the anisotropy and vanishing remanence with film thickness can be explained because the large APB density in these ultrathin films randomizes the magnetization.

To conclude, epitaxial Fe_3O_4 films grown on MgO substrates show an increased resistivity with respect to the bulk, and the resistivity increases with decreasing film thickness. The increase in resistivity can be explained by the presence of antiphase domain boundaries in the films. The thickness dependence of the resistivity is related to a significant decrease in domain size with decreasing film thickness. The relationship between the resistivity and APB structure is important for the application of these films in device structures. The effective conductivity has been modeled using the effective medium approximation. From fits to the experimental data, a value of 2 nm is found for the width of the domain boundary. The thinnest films (25 nm and below) do not show a Verwey transition. This is probably also due to the very small domain sizes, which inhibit long-range order.

---

*Corresponding author. Email address: w.eerenstein@phys.rug.nl.

[1] A. Yanase and K. Siratori, J. Phys. Soc. Jpn. **53**, 312 (1984).

[2] G.Q. Gong, A. Gupta, G. Xiao, W. Qian, and V.P. Dravid, Phys. Rev. B **56**, 5096 (1997).

[3] W. Eerenstein, T.T.M. Palstra, S.S. Saxena, and T. Hibma, Phys. Rev. Lett. **88**, 247204 (2002).

[4] X.W. Li, A. Gupta, G. Xiao, and G.Q. Gong, J. Appl. Phys. **83**, 7049 (1998).

[5] R.J.M. van de Veerdonk, M.A.M. Gijs, P.A.A. van der Heijden, R.M. Wolf, and W.J.M. de Jonge, in *Epitaxial Oxide Thin Films II*, edited by D. K. Fork, J. S. Speck, T. Shiosaki, and R. M. Wolf, Mater. Res. Soc. Symp. Proc. 401 (Materials Research Society, Pittsburgh, 1996), p. 455.

[6] M. Ziese and H.J. Blyte, J. Phys.: Condens. Matter **12**, 13 (2000).

[7] D.T. Margulies, F.T. Parker, M.L. Rudee, F.E. Spada, J.N. Chapman, P.R. Aitchison, and A.E. Berkowitz, Phys. Rev. Lett. **79**, 5162 (1997).

[8] F.C. Voogt, T.T.M. Palstra, L. Niesen, O.C. Rogojanu, M.A. James, and T. Hibma, Phys. Rev. B **57**, R8107 (1998).

[9] M.L. Rudee, D.T. Margulies, and A.E. Berkowitz, Microsc. Microanal. **3**, 126 (1997).

[10] D. Bruggeman, Ann. Phys. (Leipzig) **24**, 636 (1935).

[11] S. Torquato and S. Hyun, J. Appl. Phys. **89**, 1725 (2001).

[12] W. Eerenstein, L. Kalev, L. Niesen, T. T. M. Palstra, and T. Hibma, J. Magn. Magn. Mater. (to be published).

[13] D. Ihle and B. Lorenz, Philos. Mag. B **42**, 337 (1980).

[14] J.P. Wright, J.P. Attfield and P.G. Radaelli, Phys. Rev. Lett. **87**, 266401 (2001).

[15] P.A.A. van der Heijden, J.J. Hammink, P.H.J. Bloemen, R.M. Wolf, M.G. van Opstal, P.J. van der Zaag and W.J.M. de Jonge, in *Magnetic Ultrathin Films, Multilayers and Surfaces*, edited by A. Fert, H. Fujimori, G. Guntherodt, B. Heinrich, W. F. Egelhoff, Jr., E. E. Marinero, and R. L. White, Mater. Res. Soc. Symp. Proc. 384 (Materials Research Society, Pittsburgh, 1995), p. 27.